Modelling ammonia emission from swine slurry based on chemical and physical properties of the slurry

E.L. Cortus[1,2]*, S.P. Lemay[3], E.M. Barber[4] and G.A. Hill[5]

*[1]Department of Agricultural and Bioresource Engineering, University of Saskatchewan, Saskatoon, Saskatchewan S7N 5A9, Canada; [2]Prairie Swine Centre Inc., Saskatoon, Saskatchewan S7H 5N9, Canada; [3]Research and Development Institute for the Agri-environment, Québec, Québec G1P 3W8, Canada; [4]Office of the Provost and VP Academic, University of Saskatchewan, Saskatoon, Saskatchewan S7N 5A2, Canada; and [5]Department of Chemical Engineering, University of Saskatchewan, Saskatoon, Saskatchewan S7N 5A9, Canada. *Current Address: Agricultural and Biosystems Engineering, South Dakota State University, Brookings, South Dakota, USA, 57007. Email: Erin.Cortus@sdstate.edu.*

Cortus, E.L., S.P. Lemay, E.M. Barber and G.A. Hill. 2009. **Modelling ammonia emission from swine slurry based on chemical and physical properties of the slurry**. Canadian Biosystems Engineering/Le génie des biosystèmes au Canada **51**: 6.9–6.22.
The slurry pit is one of the main sources of ammonia emission in swine enterprises. Ammonia emission from slurry is considered a convective mass transfer process, but there are different methods to predict the mass transfer coefficient and the amount of ammonia in the gas film at the slurry surface. The objective of this research is to develop a new model to simulate the ammonia emission rate from swine slurry that can be applied to slurries of varying physical and chemical composition (i.e., pH, temperature, concentration, etc.). Slurry samples were collected from pigs fed diets differing in crude protein and sugarbeet pulp content and placed in emission boxes where the headspace ammonia concentration was measured and used to calibrate and validate a new ammonia emission rate model for slurry. The new model relates the fraction (f) of ammonia in the slurry relative to the total ammoniacal nitrogen concentration (TAN) as a linear function of pH and TAN, based on both single and multiple variable regression analyses. The average bias between the simulated and measured emission box concentration levels for seven datasets was -3%. The new model was deemed accurate for slurry with TAN concentration levels between 0.3 and 1.0 mol l^{-1}, and pH levels between 8 and 9. Because the value f is based on a linear relationship with pH, the ammonia emission rate from slurry is less sensitive to changes in pH compared with previous models that used an exponential relationship between f and pH. **Keywords:** ammonia emission, slurry, TAN, pH, mass transfer, modelling.

Le lisier des dalots est l'une des principales sources d'émissions d'ammoniac dans les exploitations porcines. L'émission d'ammoniac provenant du lisier est un processus de transfert de masse par convection et il existe différentes méthodes pour prédire le coefficient de transfert de masse et la quantité d'ammoniac dans le film gazeux à la surface du lisier. L'objectif de cette recherche est de développer un nouveau modèle pour simuler le taux d'émission d'ammoniac du lisier de porc qui peut être utilisé avec des lisiers ayant une composition physique et chimique différente (i.e. pH, température, concentration, etc.). Les échantillons de lisier prélevés provenaient de porcs nourris à une diète à base de grains et ayant différents contenus en protéine brute et en pulpe de betterave à sucre. Les échantillons étaient placés dans une chambre d'émission où la concentration en ammoniac était mesurée dans l'espace au-dessus des échantillons. Ces mesures de concentration ont été utilisées pour calibrer et valider un nouveau modèle de taux d'émission pour le lisier. Le nouveau modèle fait le lien entre la fraction (f) de l'ammoniac dans le lisier relatif à la concentration en azote ammoniacal total (TAN) en relation linéaire avec le pH et la TAN et ce basé sur des analyses de régression simple et multiple. La moyenne de l'écart entre les niveaux de concentration simulés et mesurés dans la chambre d'émission pour un ensemble de sept groupes de données était de -3%. Le nouveau modèle était considéré précis pour des lisiers ayant des niveaux de concentration de TAN compris entre 0,3 et 1,0 mol l^{-1} et des niveaux de pH variant de 8 à 9. Parce que la valeur de f est basée sur une fonction linéaire du pH, le taux d'émission d'ammoniac du lisier est moins sensible aux changements de pH comparativement aux modèles existants qui font appel à une relation exponentielle entre f et le pH. **Mots clés:** émission d'ammoniac, lisier, TAN, pH, transfert de masse, modélisation.

INTRODUCTION

The under-floor manure storage area, often referred to as the slurry pit, is recognized as one of the main sources of ammonia production within swine and cattle barns. With the steady addition of urine, feces, drinking water and spilled feed to the slurry pit, ammonia and other gases are continually formed by the breakdown of urea and other nitrogenous material such as proteins (Anderson et al. 1987). Given the highly variable nature of slurry composition and duration of storage, models that simulate the ammonia generation rate from the urea/protein breakdown within the slurry depth are still developing (Ni 1999). However, measurements of the physical (i.e., temperature) and chemical (i.e., pH, concentration) slurry properties are possible and these measured values can be used to predict the ammonia emission rate from the slurry surface for the measured conditions. By developing a model that accurately simulates the ammonia emission rate from slurry (E_S) based on measurable variables, the livestock industry will be better able to assess ammonia emission from stored slurry and design practical solutions

to reduce the impact this emission can have on human, swine, and environmental health.

Numerous models have been developed to simulate the ammonia emission from slurry surfaces either as stand-alone models or components of barn-scale emission models. The E_S models by Zhang et al. (1994), Aarnink and Elzing (1998), Ni et al. (2000) and Liang et al. (2002) all have a core model based on convective mass transfer, but differences exist among the models in mass transfer coefficients and ammonia partitioning in the solution. All four models are very sensitive to the slurry pH, which can vary greatly between manure sources (Paul and Beauchamp 1989) and even within the depths of a manure pit (Zhang et al. 1994; Aarnink and Elzing 1998; Ni et al. 2000). Of the E_S models developed, validation and calibration have been completed with either full-scale room measurements (Aarnink and Elzing 1998; Ni et al. 2000) that do not necessarily separate E_S from emission by other sources, or with lagoon storage emission data (Liang et al. 2002). Some models have considered or accounted for a change in slurry surface pH as a result of carbon dioxide emission from the slurry (Aarnink and Elzing 1998; Ni et al. 2000). However, changes in surface pH and differences between mixed and surface pH have not been validated with measured data in conjunction with model testing for these existing models. Also, the range of slurry properties that were used for model testing was limited in these existing models.

Diet composition is a large determinant in slurry composition and, therefore, slurry emission models that consider the impact of multiple slurry properties will be better suited to predict E_S for varying feed composition. For example, reducing dietary crude protein can lower the amount of nitrogen excreted in the urine and can also result in lower slurry pH and ammonia emissions (Canh et al. 1998a). Adding sugarbeet pulp to a pig's diet was found to lower the pH and ammonia emissions from slurry by increasing the volatile fatty acid concentration of the slurry (Canh et al. 1998b).

The overall objective of this experiment was to develop an E_S model to simulate the ammonia emission rate from slurry pits within swine barns that is suitable over a range of slurry chemical and physical properties, namely pH, temperature and concentration. The specific objectives to achieve the overall objective were: (1) to build on pre-existing models and develop a model to simulate the ammonia emission from slurry; (2) to collect slurry composition and emission rate measurements from slurry samples varying in composition in a bench-scale slurry pit set-up; and (3) to calibrate and validate the model using the bench-scale measurements. The calibration process focused on determining the fraction of total ammoniacal nitrogen in ammonia form, based on slurry properties that are relatively easy to measure, either on site or through commercial labs.

MODEL DEVELOPMENT

A schematic diagram of a slurry pit in relation to the slatted and solid floors is shown in Fig. 1, and forms the basis for the model development. Urine, fecal matter, spilled feed and water drain through the slatted floor and mix to become slurry. Ammonia is produced within the slurry from the breakdown of urea and other nitrogenous material. Once in solution, the ammonia exists in two forms, ammonia (NH_3) and ammonium (NH_4^+). The total amount of nitrogen in NH_3 and NH_4^+ form in a solution is referred to as the total ammoniacal nitrogen concentration (TAN). The non-ionized portion of TAN, NH_3, is volatile and can be transferred to the slurry pit headspace air, whereas the NH_4^+ will stay in the solution. Air is added and removed from the slurry pit headspace through the slatted floor. Ammonia absorption or desorption by the walls and slatted floor is neglected.

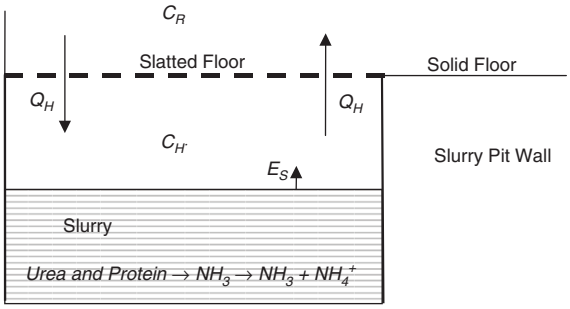

Fig. 1. Cross-sectional diagram of a slurry pit showing the contributions of ammonia to the headspace concentration (C_H) by incoming air from the room ($C_R \cdot Q_H$) and emission from the slurry (E_S), and removal of ammonia by air movement up through the slats ($C_H \cdot Q_H$).

Ni (1999) found that most models rely on convective mass transfer from slurry surfaces to predict NH_3 emission rates (Eq. 1), with sub-models to determine the convective mass transfer coefficient (k) and the NH_3 concentration in the gas film (C_G). In determining C_G, most models have predicted the ratio (f) of NH_3 to TAN in the liquid and then estimated the NH_3 concentration in the gas film relative to the liquid based on the Henry's Law constant (H). The concentration gradient for NH_3 emission is dependent on the concentration of NH_3 in the surrounding bulk air. In developing this E_S model, C_H was retained in the mass transfer equation as the concentration of the surrounding air.

$$E_S = k \cdot A \cdot 1000(C_G - C_H) = k \cdot A \cdot 1000 \cdot \left(\frac{f \cdot TAN}{H} - C_H\right) \quad (1)$$

To determine k, f and H, in order to solve Eq. 1, the models developed by Zhang et al. (1994), Aarnink and Elzing (1998), Ni et al. (2000) and Liang et al. (2002) were compared and are presented in Table 1. While all four models use a similar approach, there are differences between models in the sub-model calculations in both the overall emission rate equation (Eqs. A4 to D4) and the units of measure. The equations were converted to similar units when possible. The temperature variable refers to the

Table 1. Ammonia emission from slurry (E_S) model comparison.

	Variable calculations specific to each model			
Calculated variable	*Zhang et al. (1994)*	*Aarnink and Elzing (1998)*	*Ni et al. (2000)*	*Liang et al. (2002)*
Mass transfer coefficient (k)	$k = (5.3 \times 10^{-3} - 1.3 \times 10^{-2} \cdot v + 8.5 \times 10^{-4} \cdot v \cdot T_C + 2.3 \times 10^{-2} \cdot v^2) \cdot 1.16 \times 10^{-5}$	$k = 50.1 \cdot v^{0.8} \cdot T_{film}^{-1.4}$	$k = 4.78 \times 10^{-7} \cdot T_C^{0.8} \cdot v^{0.7}$	$k = \left(\frac{1}{k_L} + \frac{1}{H'' \cdot k_G}\right)^{-1}$ where $k_L = 2.229 \times 10^{-6} \cdot e^{0.236 \cdot v}$ $k_G = 5.317 \times 10^{-5} + 2.012 \times 10^{-3} \cdot v$
	(A1)	*(B1)*	*(C1)*	*(D1)*
Fraction of TAN in unionized form (f) or Proportionality coefficient (P_{CO})	$f = \frac{10^{pH}}{10^{pH} + \frac{1}{K_a}}$ where $K_a = 0.2 \cdot 10^{-\left(0.0897 + \frac{2729}{T}\right)}$	$f = \frac{10^{pH_E}}{10^{pH_E} + \frac{1}{K_a}}$ where $pH_E = pH + 1.1$ $K_a = 0.2 \cdot 10^{-\left(0.0897 + \frac{2729}{T_{film}}\right)}$	$P_{CO} = \frac{K_a}{(q \cdot 10^{-pH_i} + K_a) \cdot H}$ where $K_a = 10^{-0.0897 - \frac{2129}{T}}$	$f = \frac{K_a}{K_a + 10^{-pH}}$ where $K_a = 0.5 \cdot 10^{-\left(0.0897 + \frac{2729}{T}\right)}$
	(A2)	*(B2)*	*(C2)*	*(D2)*
Henry Constant (H)	$H' = \frac{P_G}{C_L}$ $H' = 1.1561 \cdot e^{-\frac{4151}{T}}$	$H = \frac{C_L}{C_G}$ $H = 1431 \cdot 1.053^{(293 - T_{film})}$	$H = \frac{C_L}{C_G}$ $H = 10^{\frac{1478}{T} - 1.69}$	$H'' = \frac{C_G}{C_L}$ $H'' = \frac{2.395 \times 10^5}{T} \cdot e^{\left(-\frac{4151}{T}\right)}$
	(A3)	*(B3)*	*(C3)*	*(D3)*
*Overall Emission (E_S)**	$E_S = k \cdot A \cdot \left(\frac{f \cdot TAN}{H'} - C_B\right)$	$E_S = \frac{k \cdot A \cdot f \cdot TAN}{H}$	$E_S = k \cdot A \cdot \left(\frac{17}{18} \cdot P_{CO} \cdot TAN - C_B\right)$	$E_S = k \cdot A \cdot f \cdot TAN$
	(A4)	*(B4)*	*(C4)*	*(D4)*

NOTE: Care has been taken to convert all models to similar variables, and it is not the authors' intention to misrepresent previous models.
*Unit conversion may be necessary to properly solve E_S.

temperature of the slurry, except where the film temperature is specified.

Convective mass transfer coefficient

In a review paper, Ni (1999) listed the wide range of convective mass transfer coefficients used for agricultural ammonia sources. The experimental values ranged from 1.3×10^{-6} to 11.7×10^{-3} m s^{-1}, and there was a positive relationship for the coefficient with temperature and air velocity. Zhang et al. (1994) and Ni et al. (2000) used experimental mass transfer coefficients to develop their respective models, shown as Eqs. A1 and C1 in Table 1, respectively. For theoretical calculations of the mass transfer coefficient, two main theories are used (Ni 1999). Aarnink and Elzing (1998) and Liang et al. (2002) base the mass transfer coefficient calculation on the Two-Film Theory proposed by Lewis and Whitman (1924). For this theory, the conductivities of the liquid (k_L) and gas (k_G) films at the emission surface are measured and combined in the overall coefficient (see Eq. D1 in Table 1 as an example). The individual film coefficients used by Liang et al. (2002) were derived from Liss and Slater (1974) (Eq. D1 in Table 1). Aarnink and Elzing (1998) use the gas film coefficient (k_G) measured by Haslam et al. (1924) as the overall mass transfer coefficient (Eq. B1 in Table 1).

The other theory that has been applied is the Boundary Layer Theory (Ni 1999), which is described in Incropera and DeWitt (1996). The mass transfer coefficient is based on the properties of the gas flowing over a flat surface of length L for laminar ($Re < 5 \times 10^5$; Eq. 2) or transitional/turbulent flow ($Re > 5 \times 10^5$; Eq. 3).

$$k = \frac{0.664 \cdot \mathrm{Re}^{0.5} \cdot Sc^{0.333} \cdot D_{A,B}}{L}, Sc \geq 0.6 \quad (2)$$

$$k = \frac{0.0296 \cdot \mathrm{Re}^{0.8} \cdot Sc^{0.333} \cdot D_{A,B}}{L}, 0.6 < Sc < 3000 \quad (3)$$

The Re and Sc parameters (dimensionless) are functions of surface length, velocity, kinematic viscosity and diffusivity. Kinematic viscosity of air (υ) can be expressed as a function of film temperature using the regression equation shown in Eq. 4, developed from data in Incropera and DeWitt (1996). Film temperature is assumed to be equal to the average temperature of the solution surface and surrounding air (Incropera and DeWitt 1996).

$$\upsilon = 4 \times 10^{-10} \cdot T_{film}^{1.859} \quad (4)$$

Diffusivity also exhibits an exponential relationship with temperature, shown in Eq. 5, adapted from Welty et al. (1984), assuming the collision interval effects at different temperatures are negligible.

$$D_{A,B}|_{T_2} = D_{A,B}|_{T_1} \cdot \left(\frac{T_2}{T_1}\right)^{1.5} \quad (5)$$

Incorporating Eqs. 4 and 5 into Eq. 2, an equation to express k as a function of velocity, temperature, length and diffusivity was developed. Equation 6 is applicable for the transfer of a substance A, from a liquid surface to the surrounding air (substance B), provided there are laminar flow conditions, the Sc value is approximately equal to or greater than 0.6, and the diffusivity of substance A in air at 298 K is known.

$$k = 0.0821 \cdot T_{film}^{0.70} \cdot v^{0.5} \cdot D_{A,B}^{0.66} \cdot L^{-0.5} \quad (6)$$

Diffusivity of ammonia in air at 298 K is 0.28×10^{-4} m^2 s^{-1} (Incropera and DeWitt 1996).

Ammonia partitioning in the liquid

The ammonia produced within the slurry will separate and exist in two forms, NH_3 and NH_4^+. Typical chemical analyses of liquid samples, however, can only provide a measure of TAN. Because only the NH_3 fraction of the TAN is volatile, Zhang et al. (1994) introduced a variable (f) to express the amount of NH_3 relative to TAN.

$$f = \frac{[NH_3]}{[NH_3 + NH_4^+]} = \frac{[NH_3]}{TAN} \quad (7)$$

Theoretically, the amounts of NH_3 and NH_4^+ in solution are in equilibrium according to Eq. 8 (Arogo et al. 2003), where K_a represents the dissociation constant for NH_4^+ and φ represents the activity coefficient of the respective ion.

$$K_a = \frac{\varphi_{NH3} \cdot [NH_3] \cdot \varphi_{H+} \cdot [H^+]}{\varphi_{NH4} \cdot [NH_4^+]} \quad (8)$$

The temperature-dependency of K_a for NH_4^+ in water was modelled by Jayaweera and Mikkelsen (1990) (Eq. 9).

$$K_a = 10^{-\left(0.0897 + \frac{2729}{T_{film}}\right)} \quad (9)$$

The activity coefficients (φ) are a function of the ionic strength of the solution, and normally assumed equal to one for dilute solutions (Arogo et al. 2003). However, a factor that theoretically represents the combination of activity values has been combined with the K_a for NH_4^+ in water to estimate K_a for NH_4^+ in manure. Zhang et al. (1994) and Aarnink and Elzing (1998) used a factor of 0.2, Liang et al. (2002) used a factor of 0.5, while Arogo et al. (2003) suggested factors between 0.50 and 0.94 based on the temperature of the slurry solution. Arogo et al. (2003) concluded that more studies are required to determine K_a values for slurry with different TAN concentrations and solid contents.

In the models of Zhang et al. (1994), Aarnink and Elzing (1998) and Liang et al. (2002), the f-variable was calculated by rearranging Eq. 8 to express the NH_4^+ concentration as a function of the NH_3 concentration, H^+ concentration and K_a, and substituting the expression into Eq. 7. The resulting equation for f was then expressed as a function of pH (negative logarithm of H^+) and K_a with a corresponding factor ranging from 0.2 to 0.5, as shown in Eqs. A2, B2 and D2. The resulting f variables have an exponential relationship with pH and, as shown in

Aarnink and Elzing (1998), a small increase in slurry pH (0.1 unit) resulted in a large increase (9%) in the simulated NH_3 emission from a barn because of the higher amount of NH_3 available.

A K_a-factor less than one reduces the impact of pH on the partitioning of NH_3 in the liquid and the resulting emission but, as shown by Arogo et al. (2003), this factor can be highly variable depending on the physical and chemical properties of the slurry. Therefore, this model will assume that f is better estimated from some measured chemical and physical properties. While there are numerous measurable properties, this paper will focus on TAN, pH, electrical conductivity (EC) and T_{film} measurements. Electrical conductivity can provide an estimate of the amount of dissolved ions in a solution (Sawyer and McCarty 1978). A linear regression equation (Eq. 10) was proposed that estimates f based on TAN, pH, EC and T_{film}, with the coefficients $x_{1\ldots5}$ determined in the model calibration process.

$$f = x_1 \cdot TAN + x_2 \cdot pH + x_3 \cdot EC + x_4 \cdot T_{film} + x_5 \qquad (10)$$

Ammonia concentration in the gas film

Another estimate in E_S models is the amount of NH_3 in the gas layer at the surface of the manure. Treybal (1980) recommended applying the Henry's Law constant for TAN concentrations in water below 3.2 mol L^{-1} at 10°C and 2.0 mol L^{-1} at 30°C. Numerous equations have been developed to express the Henry's constant for ammonia emission models with different dimensions and definitions (Ni 1999). Table 1 demonstrates that previous E_S models have expressed the Henry's constant as either as the dimensionless ratio of NH_3 in the liquid compared to the gas (H, Eqs. B3 and C3 in Table 1), the ratio of partial pressure to liquid concentration (H', Eq. A3 in Table 1), or the dimensionless ratio of ammonia in the gas compared to the liquid (H'', Eq. D3 in Table 1). Ni (1999) concluded the Henry's constant for ammonia emission modelling is "currently in a state of confusion and a standard Henry's constant needs to be established"; in the meantime Ni (1999) recommended using H for E_S models because the NH_3 concentration in the surrounding air is generally expressed as a concentration, rather than a partial pressure. The Henry's constant calculation from Aarnink and Elzing (1998) was used in this E_S model (Eq. 11).

$$H = \frac{C_L}{C_G} = 1431 \cdot 1.053^{(293 - T_{film})} \qquad (11)$$

Ammonia concentration in the slurry pit headspace

If high enough, the NH_3 concentration in the slurry pit headspace (C_H) can impact the concentration gradient for E_S. Assuming the slatted floor above the slurry pit acts as a conduit for incoming air to the headspace and for outgoing air, the dynamic concentration of the headspace is shown in Eq. 12.

$$\frac{dC_H}{dt} = \frac{Q_H \cdot C_R - Q_H \cdot C_H + E_S}{V_H}$$

$$= \frac{Q_H \cdot C_R - Q_H \cdot C_H + k \cdot A \cdot 1000 \cdot \left(\frac{f \cdot TAN}{H} - C_H\right)}{V_H} \qquad (12)$$

If the headspace concentration can be considered at steady state because of its relatively large capacity, and assuming the incoming air has a negligible NH_3 concentration, Eq. 12 can be simplified to the static model shown in Eq. 13.

$$C_H = \frac{k \cdot A \cdot 1000 \cdot f \cdot TAN}{H \cdot (Q_H + k \cdot A \cdot 1000)} \qquad (13)$$

Model development summary

With input values for T_{film}, v, TAN, pH, EC and A, the emission rate from slurry can be calculated using Eq. 6 to determine the mass transfer coefficient, Eq. 10 to estimate f, Eq. 11 to calculate the Henry's Law constant, all incorporated in Eq. 1 to simulate the NH_3 emission rate. For slurry contained within an enclosed space like a slurry pit, the concentration of the slurry pit headspace can be estimated using the most recent measurement or simulated value, and the air exchange rate Q_H (Eq. 13).

DATA COLLECTION and ANALYSIS

Data for input, calibration and validation of the developed E_S model were collected from slurry samples produced by individual pigs in conjunction with another experiment (Smith et al. 2004). The slurry was placed in emission boxes designed to simulate a slurry pit environment with low airspeed and a low air exchange rate, where the NH_3 concentration in the emission box headspace (C_B) was analogous to the slurry pit headspace concentration (C_H), and the air exchange rate through the emission box (Q_B) was analogous to the air exchange rate through the slatted floor (Q_H) of slurry pit. Measurements collected from the slurry and from within the emission boxes provided the data needed for input to the model, and for calibration and validation of the model.

Slurry collection

Two metabolism trials were performed with average pig masses of 58 (Trial 1, dataset 2) and 94 kg (Trial 2, dataset 1), respectively. For each trial, four different diet formulations were prepared and are explained in greater detail in Smith et al. (2004). Two pigs in each trial were given the same diet treatment. The four treatments were low protein, with and without sugarbeet pulp added as a form of fermentable carbohydrates (LPSBP and LPC, respectively), and high protein, with and without sugarbeet pulp (HPSBP and HPC, respectively). An 18-day acclimation period was provided for the animals to adjust to the experimental diets before slurry collection.

Pigs were housed individually in metabolism crates with a cone-shaped metal tray under the slatted floor of each pen. The cone of the tray was plugged with a rubber stopper and all urine and feces were collected together for two (Trial 2) to four days (Trial 1). Water spillage from the drinker was collected separately, so the slurry samples were highly concentrated mixtures of urine and feces only. After the collection period for each trial, the slurry from one pen was emptied into a bucket and mixed with a paint stirrer. From the mixed slurry, an 8-L sample was taken and put into an emission box. This procedure was repeated with the slurry from all eight pigs during each of the two trials.

Emission box measurements

The slurry samples were placed in emission boxes constructed from 17-L Rubbermaid containers (Wooster, OH) lined with Tedlar bags to prevent gas and odour absorption as shown in Fig. 2. The lid was sealed to the box before measurements were taken.

Air entered each emission box through a series of 7 holes (13.5-mm diameter) on one end of the box, 12.7 mm above the slurry surface. Teflon tubing from the outlet on the other end of each chamber was connected to the NH_3 measurement system. Ambient NH_3 concentration was also measured. The NH_3 measurement system consisted of a sampling pump that drew air through one sampling line at an average rate of 0.05 L s^{-1} (Model 013-88ST; Aalborg Instruments, Orangeburg, NY) into a mixing manifold from which the NH_3 analyzer (Chillgard RT refrigerant monitor, MSA Canada, Edmonton, AB; range 0 to 1000 ppm; accuracy ± 2 ppm) and other gas sampling equipment (not used as part of this study) could continuously draw the required amount of air for analysis. A second pump continually purged the remaining eight lines at a similar average flowrate (Model GF-1560; Gilmont Instruments, Barrington, IL). A programmable logic controller (Septre Controls Ltd., Regina, SK) coordinated the sampling of different emission boxes by switching the sampled line every ten minutes between the emission boxes and/or ambient. The first 6 min of data for every 10-min sampling period were considered stabilizing time during which the previous air sample was fully replaced with the current air sample in the manifold and analyzer, and thus discarded; only data from the last 4 min of the 10-min sampling period were saved and used to compute an average concentration. A dust filter was installed at the inlet to the sampling line in each box to prevent particulate contamination of the line or analyzers.

Temperatures of the slurry surface and airspace in the box were continuously measured (Type T Thermocouple, temperature accuracy: ± 0.5°C) and averaged to determine the film temperature at 10-min intervals.

Air velocity measurements within the boxes were taken after the emission trials were completed, 5 mm above the liquid surface, with a thermal anemometer (TSI Model 8470 Air Velocity Transducer, St. Paul, MN). The range of the anemometer was 0 to 0.5 m s^{-1} and the instrument was calibrated in a bench-top wind tunnel (Model 8390, TSI Incorporated, St. Paul, MN). The velocity was measured at nine locations in each box. Within each individual box, the velocity measurements at the nine locations did not differ more than 10% from the average box velocity measurement. The range of average box velocity measurements for all boxes was 0.019 to 0.041 m s^{-1}. An average velocity of 0.025 m s^{-1} was used in all calculations. A sensitivity analysis (shown in the Results section) showed that the average velocity under- or over-predicted the concentration by less than 10% based on the range measured.

Before each trial the boxes were rinsed with bleach solution and water and fumigated. The empty boxes were measured for any NH_3 absorption using the same method as the experiments over 24 h, and it was found that the NH_3 concentration in the boxes was less than 1 ppm different from the ambient concentration.

Experimental procedure

The slurry collected from the eight pigs during each slurry collection period was placed in emission boxes, which were stored in an instrumentation room. The measured headspace concentrations exceeded the limit of the NH_3 analyser (1000 ppm) when first measured. The experimental procedure was altered slightly to accommodate this. For each slurry sample in both trials, the NH_3 was allowed to volatilize from the slurry samples for 8 (Trial 1) and 6 (Trial 2) days until the NH_3 concentration levels for all boxes were below 1000 ppm. The slurry was emptied into a bucket and remixed with the paint stirrer before being placed back in the box. A 1-L slurry sample was

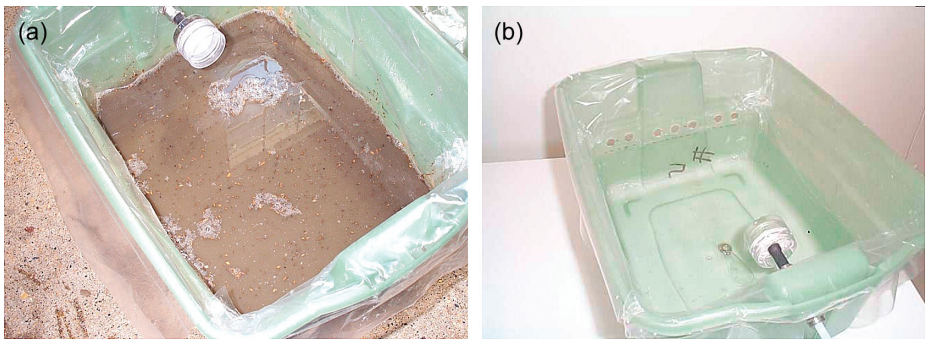

Fig. 2. Emission box, filled with slurry (a) and inside view (b).

taken at this time, referred to as the day 0 sample, and analyzed for TAN, pH and *EC*. After measuring the NH_3 emission for another 5 days, the emission trials were considered complete and another slurry sample was taken, referred to as the day 5 sample, and analyzed for TAN, pH and *EC*. Slurry samples were analysed by an independent laboratory. Chemical properties between day 0 and day 5 for each sample were linearly interpolated.

The emission box concentration data from the HPC diet slurry (Rep 2) in dataset 2 was discarded entirely because of a hole discovered in the gas sampling line. Power outages occurred in both trials, resulting in the loss of some NH_3 concentration measurements.

Data analysis

Eight slurry samples were used in each of two trials, with four treatments replicated twice in each trial. The animal diets are considered the treatments, and will be referred to as HPC, HPSBP, LPC and LPSBP.

Concentration data were used in the data analysis. Dataset 1 samples were used for calibration, and dataset 2 samples were used for validation. The emission boxes were designed to simulate the slurry pit environment, so C_H, V_H and Q_H in Eqs. 12 and 13 of the E_S model were replaced with the emission box concentration (C_B), emission box volume (V_B), and emission box air exchange rate (Q_B), respectively. Preliminary calculations using Eqs. 12 and 13 to simulate the emission box concentration levels with input values collected in dataset 1 were similar in magnitude for calculation intervals less than 2 h, prompting the use of the simpler, steady state equation (Eq. 13).

The calibration process using dataset 1 samples was as follows: (1) Eq. 13 was rearranged to solve for *f*, based on the measured airspace (C_B), slurry TAN values and other airflow conditions; (2) an average value for *f* was obtained for each of the samples based on the measured air properties and TAN values throughout the trial; (3) single and multi-variable regression was then performed to express *f* as a function of different combinations of measured slurry property values (Eq. 10); and finally, (4) regression equations were evaluated based on their statistical significance to determine the appropriate expression for *f*. All calculations were performed using MSExcel®.

During the validation process, the calibrated equation for *f* was incorporated into Eq. 13 [hereafter referred to as the Linear-pH (Lin-pH) Model], and the simulated air concentration values for each dataset 2 sample were compared to measured air concentration values over time. The two largest changes to the Lin-pH Model compared with previous models were a different *k* estimation (Eq. 6) and a linear relationship between pH and *f*. To evaluate the improvement these two changes made to the simulation process, the Lin-pH Model was compared with a second model that also used Eq. 13 to calculate the emission box concentration, but estimated *k* and *f* using Eqs. A2 and B1 (from Table 1), respectively. Equation A2 represents the Two-Film Theory *k*-calculation and Eq. B1 represents the exponential-type relationship between *f* and slurry pH. The second model was referred to as the Exponential-pH (Exp-pH) Model. Both the Lin-pH and Exp-pH Models were evaluated following the Standard Guide for Statistical Evaluation of Indoor Air Quality Models (ASTM 2003). The evaluation parameters and the suggested limits of the ASTM (2003) standard are: (1) correlation coefficient, $R > 0.9$; (2) line of regression with a slope (b) between 0.75 and 1.25, and an intercept (a) less than 25% of the average measured concentration; (3) normalized mean square error, NMSE < 0.25; (4) fractional or normalized bias of the mean concentrations, $-0.25 <$ FB < 0.25; and (5) bias based on the variance of the concentrations, $-0.5 <$ FS < 0.5 (ASTM 2003). Finally, a sensitivity analysis was performed using both the Lin-pH and Exp-pH models to investigate the effects of different input variables on the simulated E_S using Eq. 1. The method used in this sensitivity analysis was as follows:

1. A mean value was set for the four input variables (T_{film}, *v*, TAN and pH) to the E_S model.
2. Leaving *v*, TAN and pH at their mean values, the input value for T_{film} was varied from 80, 90, 110 and 120% of its mean value, and the corresponding value for E_S calculated using the Lin-pH and Exp-pH models.
3. Using $T_{film} = 293$ K (or 80% of the mean value for T_{film}) as an example, a percent change in E_S (for both the Lin-pH and Exp-pH models) was calculated based on the difference between $E_{S,\ Tfilm=293}$ and $E_{S,\ Tfilm=298}$, relative to $E_{S,\ Tfilm=298}$.
4. Steps 1 to 3 were repeated for each input variable.

RESULTS and DISCUSSION

Slurry properties

Table 2 shows the measured TAN, pH and *EC* measurements on days 0 and 5 for the 16 slurry samples. There was a substantial change in the properties of the dataset 1 LPC (1) sample that was not seen in other samples, suggesting this particular sample was an anomaly and possible outlier. There was not a discernable relationship between TAN and pH, as one would expect in a pure NH_3 and water solution, likely because other components in the manure were buffering the pH. In a pure NH_3 solution, the pH increases as TAN concentration increases because NH_3 is a weak base.

The TAN concentrations of the slurry samples were higher than reported slurry TAN concentration levels in the literature, likely because the urine and feces were combined with no dilution. Based on the slurry analysis results (Table 2), lowering the crude protein and adding sugarbeet pulp to the diet composition did not result in the expected changes to TAN and pH, as was seen in Canh et al. (1998a,b). Even though the diet treatments did not produce the expected changes in TAN and pH, the resulting slurry showed a large variability in the slurry composition, enabling calibration of the model equations with variable sets of data. Also, the E_S measurements and developed E_S model may not cover the typical slurry conditions for all slurry pits, but the model development does still have some important implications for E_S models for slurry pits in swine barns.

Table 2. Measured slurry properties* on days 0 and 5 for the respective trials and treatments.

			TAN (mol L^{-1})		*pH*		*EC (mS cm^{-1})*	
Dataset	*Treatment***	*Rep*	*Day 0*	*Day 5*	*Day 0*	*Day 5*	*Day 0*	*Day 5*
1	*HPC*	*1*	*0.66*	*0.59*	*9.1*	*8.9*	*39.8*	*34.1*
	HPC	*2*	*0.81*	*0.74*	*9.1*	*9.0*	*43.6*	*38.4*
	HPSBP	*1*	*0.62*	*0.55*	*8.8*	*8.7*	*31.2*	*31.7*
	HPSBP	*2*	*0.41*	*0.38*	*8.5*	*8.5*	*26.3*	*24.8*
	LPC	*1*	*0.55*	*1.05*	*8.7*	*8.1*	*21.9*	*33.0*
	LPC	*2*	*1.11*	*1.08*	*8.6*	*8.4*	*42.3*	*39.4*
	LPSBP	*1*	*0.32*	*0.28*	*8.7*	*8.7*	*18.1*	*20.7*
	LPSBP	*2*	*1.11*	*1.10*	*8.5*	*8.0*	*40.5*	*34.9*
2	*HPC*	*1*	*0.37*	*0.32*	*8.8*	*9.1*	*26.8*	*22.8*
	HPC	*2*	*0.49*	*0.47*	*8.7*	*9.2*	*33.4*	*30.4*
	HPSBP	*1*	*0.47*	*0.42*	*8.0*	*8.5*	*27.0*	*32.8*
	HPSBP	*2*	*1.10*	*1.04*	*8.8*	*9.1*	*44.7*	*46.8*
	LPC	*1*	*1.01*	*0.98*	*7.7*	*8.0*	*43.8*	*43.3*
	LPC	*2*	*0.64*	*0.54*	*8.4*	*8.6*	*44.3*	*37.9*
	LPSBP	*1*	*0.66*	*0.56*	*8.4*	*8.7*	*33.8*	*35.4*
	LPSBP	*2*	*1.17*	*1.07*	*8.4*	*8.6*	*40.2*	*44.4*

*TAN, total ammoniacal nitrogen concentration; *EC*: Electrical conductivity.
**HPC, high protein; HPSBP, high protein with sugarbeet pulp; LPC, low protein; and LPSBP, low protein with sugarbeet pulp.

Ammonia concentration measurements of emission boxes

The airspace concentrations in the emission boxes were high, even after the slurry was allowed to volatilize for a number of days. The air concentrations were on average between 250 and 820 ppm, with no discernable difference between datasets 1 and 2 (Fig. 3).

Model calibration

The fraction (f) of TAN as NH_3 for each slurry sample in dataset 1 was calculated and the average value is shown in Table 3 with the corresponding average slurry properties. The calibration process showed that the relative amount of available nitrogen (f) was consistently between 3 and 9% despite the large variation in the slurry pH. The reduction in f for slurry samples at a given pH compared with TAN in water solutions has been attributed to the ionic strength of the slurry and the subsequent impact on the activity coefficients (Arogo et al. 2003). Another explanation for the reduction in f at higher pH levels may be the result of ammonia in the slurry buffering other acidic compounds. Sommer and Husted (1995) showed that slurry samples (cattle, pig, raw biogas and digested biogas slurry) exhibited elevated buffering capacities between pH levels of 8.5 and 10.5. Theoretically, the TAN content of the slurry may provide the majority of the buffering capacity in this range so that, as acidic compounds are produced, some of the ammonia is consumed. The end result would be an f-value lower than that predicted using a K_a-based equation.

Using an empirical equation to determine f based on measurable properties appears justified for the concentrated manure used in this study, since the unknown components and high variability limited the application of the K_a equation for NH_4^+ in water (Eq. 9). Solving for a K_a-factor would not have been suitable with these data, as was done by Arogo et al. (2003), since there was not a strong exponential relationship of the average f values with slurry pH.

Single variable linear regression was performed for the f values shown in Table 3 as a function of TAN, pH, *EC* and T_{film} (Eq. 10). All regressions were performed with and without the LPC (1) sample that was suspected to be

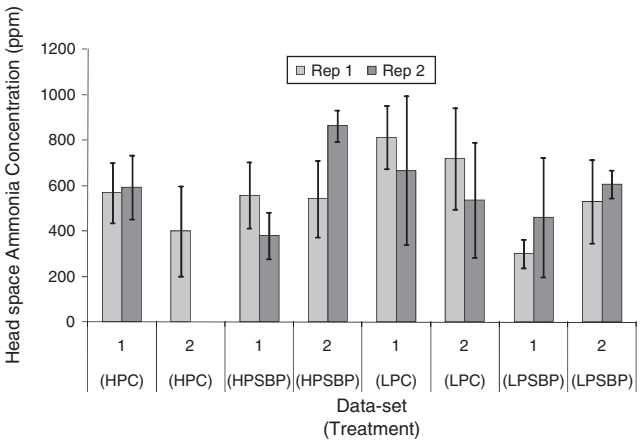

Fig. 3. Average ammonia concentration measured in the headspace of the emission boxes during the two trials. Vertical bars indicate the range of measured concentration values for the emission box during the trial. [Sample HPC(2) during Rep 2 was discarded because of a problem with the sampling line.]

Table 3. Average slurry properties and fraction (*f*) values for dataset 1 slurry samples.

							f	
Diet	*Rep*	*n**	T_{film} *(K)*	*TAN (mol* l^{-1}*)*	*pH*	*EC (mS* cm^{-1}*)*	*Mean*	*SD***
HPC	*(1)*	*45*	*297.7*	*0.63*	*9.0*	*37.1*	*0.068*	*0.008*
HPC	*(2)*	*44*	*297.3*	*0.78*	*9.1*	*41.2*	*0.058*	*0.007*
HPSBP	*(1)*	*42*	*298.5*	*0.59*	*8.8*	*31.4*	*0.068*	*0.006*
HPSBP	*(2)*	*43*	*297.5*	*0.40*	*8.5*	*25.6*	*0.073*	*0.009*
LPC	*(1)*	*43*	*297.5*	*0.78*	*8.4*	*27.0*	*0.084*	*0.024*
LPC	*(2)*	*45*	*297.3*	*1.10*	*8.5*	*40.9*	*0.047*	*0.011*
LPSBP	*(1)*	*45*	*297.3*	*0.30*	*8.7*	*19.3*	*0.077*	*0.006*
LPSBP	*(2)*	*45*	*296.9*	*1.10*	*8.3*	*37.9*	*0.033*	*0.009*

**n*, number of simulated values.
**SD, standard deviation.

an anomaly; removing the sample provided a better fit for most models. The single variable TAN best modelled the variable *f* ($R = 0.955$, $F_{1,5} < 0.001$).

Multiple regression was then performed with combinations of TAN and other measured variables. By incorporating TAN and pH in the regression Eq. 10, the intercept (x_5) was no longer significantly different from zero and was set to zero ($R = 0.974$, $F_{2,5} = 0.002$). Similarly, adding the variable temperature to the regression equation negated the need for the intercept in the regression equation ($R = 0.968$, $F_{2,5} = 0.003$). The regression equation incorporating TAN and pH (Eq. 14) was chosen as the model to predict *f* considering the higher R-value and the likelihood of a functional relationship with TAN and pH. Equation 14 is therefore applicable for swine slurry with an average TAN concentration between 0.3 and 1.1 mol l^{-1}, and pH between 8.3 and 9.1.

$$f = -0.0444 \cdot TAN + 0.00105 \cdot pH \quad (14)$$

Model validation

The ammonia concentration for each of the dataset 2 samples was calculated using Eq. 14 in Eq. 13 (Lin-pH Model) for the same instances that measured concentration values were available. A second set of model calculations were performed for the same instances using the Exp-pH Model. Sample HPC (2) was not collected due to an experimental problem. The corresponding measured and simulated concentration values were compared and evaluated for both the Lin-pH Model and Exp-pH Model, and are shown in Tables 4 and 5, respectively.

The correlation coefficient (R), normalized mean square error (NMSE) and fractional bias (FB) were within the prescribed evaluation limits for the majority of slurry samples using the Lin-pH Model (Table 4). The FB values show the average simulated concentration for each sample was between 23% lower and 11% higher than the average measured concentration. The average NMSE value was 0.0293, which is approximately equal to a normalized standard error of 17%. The Lin-pH Model shows improvement compared with the Exp-pH Model (Table 5), where the average simulated concentration was over 100% lower and higher than the measured concentration in some cases.

Each set of ammonia concentration measurements showed some diurnal variation that generally decreased in magnitude over the trial. The diurnal variation was

Table 4. "Lin-pH Model" evaluation based on dataset 2 slurry sample measurements. *Italicized* values are outside of the prescribed evaluation limits (ASTM 2003).

			Overall Agreement				Bias	
Diet	Rep	*n*	R	b	a	NMSE	FB	FS
HPC	(1)	31	0.985	*0.471*	*235*	0.0324	0.06	*−1.26*
HPSBP	(1)	29	0.899	*0.595*	*176*	0.0146	−0.08	*−0.78*
HPSBP	(2)	13	*0.784*	*0.383*	*354*	0.0556	−0.23	*−1.23*
LPC	(1)	21	*0.956*	*0.328*	*360*	0.0544	−0.19	*−1.58*
LPC	(2)	28	0.992	*0.540*	*311*	0.0297	0.11	*−1.09*
LPSBP	(1)	29	0.981	*0.672*	*234*	0.0179	0.11	*−0.72*
LPSBP	(2)	13	0.959	0.833	108	0.0007	0.01	*−0.28*
Average			0.937	0.546	254	0.0293	−0.03	*−0.99*

Table 5. "Exp-pH Model" evaluation based on dataset 2 slurry sample measurements. *Italicized* values are outside of the prescribed evaluation limits (ASTM 2003).

			Overall Agreement				Bias	
Diet	Rep	*n*	R	b	a	NMSE	FB	FS
HPC	(1)	31	*0.807*	*0.281*	*376*	0.0888	*0.20*	*−1.57*
HPSBP	(1)	29	*−0.677*	*−0.213*	*277*	*1.7959*	*−1.08*	*−1.64*
HPSBP	(2)	13	*0.661*	*1.267*	*307*	0.2432	*0.48*	*1.14*
LPC	(1)	21	*−0.082*	*−0.007*	139	*3.7253*	*−1.37*	*−1.97*
LPC	(2)	28	*0.978*	*0.341*	*162*	*0.2591*	*−0.44*	*−1.57*
LPSBP	(1)	29	*0.749*	*0.232*	*237*	0.2035	*−0.38*	*−1.65*
LPSBP	(2)	13	*0.948*	*1.431*	*−356*	0.0319	*−0.17*	*0.78*
Average			*0.483*	*0.476*	*163*	*0.9068*	*−0.39*	*−0.93*

attributed to changing temperature patterns over each 24-h period since the instrumentation room where the emission boxes were stored did not have constant temperature control. Fig. 4 shows the individual data points for all Trial 2 slurry samples used to evaluate the model simulations to the measured concentration values. Each data point represents a 4-min average collected every 90 min. The regression slope and intercept for all individual samples are not within the ASTM-suggested limits (Table 4), suggesting the variation in NH_3 concentration throughout the trial was not as well simulated as the overall average concentration for each sample.

The main differences between the Lin-pH Model and all previous models studied (Table 1) lie in the choice of mass transfer coefficient and the determination of available NH_3 in the liquid. The fractional bias in simulating the emission box NH_3 concentration appears significantly improved by using the Lin-pH Model, especially at lower pH values compared with the Exp-pH Model (Figs. 5 and 6). Figures 5 and 6 also show that the largest error in model simulations with the Lin-pH Model occurred in samples with values of TAN greater than 1.0 mol L^{-1} and pH values less than 8.3 and greater than 9.1, which are consistent with the minimum/maximum range of input values used in the development of the Lin-pH model (Eq. 14).

It will be useful to repeat these measurements over a wider temperature range and with diluted slurry to see if there is a minimum value for the amount of TAN available as NH_3. In doing so, it may be possible to replace the statistical equation for f (Eq. 14) with a mechanistic equation that better explains how the physical and chemical properties of the slurry affect the NH_3 partitioning within the slurry. In the meantime, for concentrated slurries with TAN concentrations between 0.3 and 1.1 mol L^{-1} and pH between 8.3 and 9.1, Eq. 14 provides a simple equation to determine f, based on obtainable measurements that can be used when predicting emission from urine/feces mixtures.

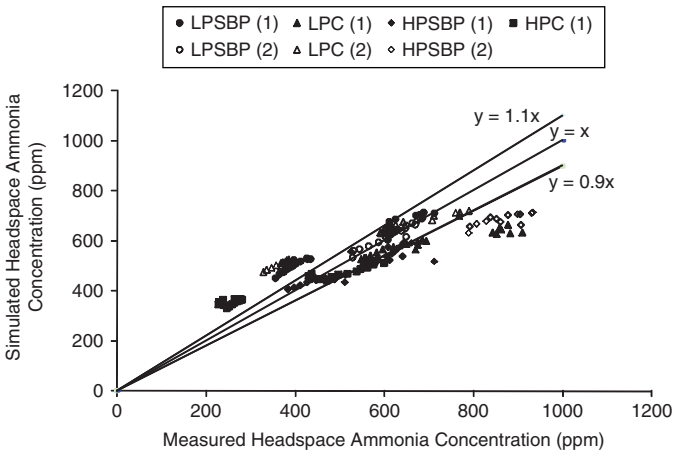

Fig. 4. Simulated ammonia concentrations compared to measured values for dataset 2 slurry samples. Each point represents a 4-min average concentration collected every 90 min.

Sensitivity analysis

The sensitivity of the emission rate calculation to the input variables T_{film}, v, TAN and pH by both the Lin-pH and

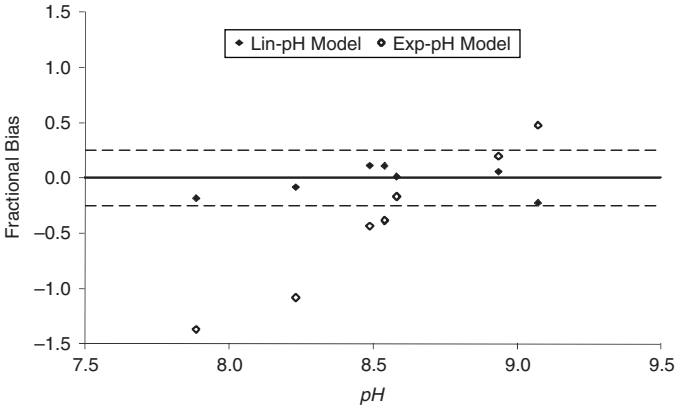

Fig. 5. Fractional bias (*FB*) of the Lin-pH and Exp-pH Model simulations of box concentration as a function of pH. Dashed lines represent recommended limits (ASTM 2003) for *FB*.

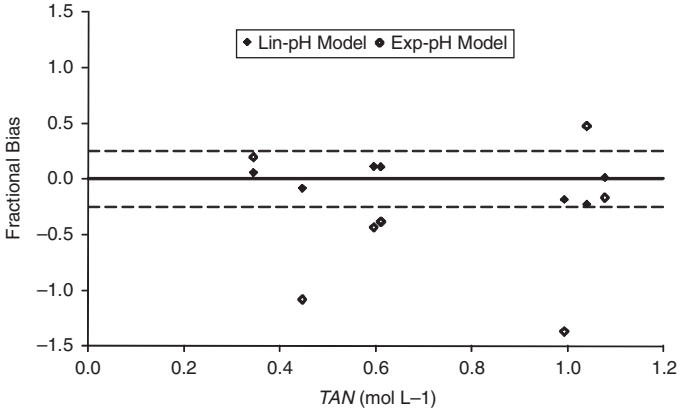

Fig. 6. Fractional bias of the Lin-pH and Exp-pH Model simulations of box concentration as a function of TAN. Dashed lines represent recommended limits (ASTM 2003) for *FB*.

Exp-pH Models is shown in Table 6. For the same input variable values, the average emission rate was lower using the Exp-pH model compared with the Lin-pH model.

Temperature has a large impact on the emission rate calculations for both the Lin-pH and Exp-pH models. In the Lin-pH model, an increase in temperature results in a higher mass transfer coefficient and thus a higher emission rate. In the Exp-pH model, an increase in temperature decreases the mass transfer coefficient (Eq. A1), but the emission rate still increases because of the strong positive relationship between f and T shown in Eq. B1.

Changing the variable v had the smallest impact in both models compared with other variables and, again, the effect was smaller with the Lin-pH Model because of the differences in mass transfer coefficient determination for the Lin-pH model (Eq. 5.6) and the Exp-pH model (Eq. B1).

The Lin-pH Model shows a reduced sensitivity to TAN compared to the Exp-pH Model, and this is attributed to the negative relationship between f and TAN, as shown in Eq. 5.14.

The relative effect of pH is significantly larger on the emission rate calculations with the Exp-pH model. For every 0.1 unit increase in pH from 8.8, the Lin-pH model estimates a 48% increase in emission whereas the Exp-pH model estimates a 1% increase in emission.

Harper et al. (2000) found the NH_3 emission rate from an anaerobic lagoon system for a swine facility to exhibit a positive, *linear* relationship with air velocity, temperature, pH and NH_4^+ concentration; slurry NH_3 concentration and pH had lower statistical influence on the NH_3 emission rate compared with air speed and temperature. Based on the sensitivity analysis, the Lin-pH E_S model was most sensitive to changes in film temperature and TAN concentration compared with the expected range of conditions for all other model variables.

With further understanding of how NH_3 emission occurs, we will better understand the contribution of the slurry pit to overall barn emissions, and we will be better able to identify NH_3 control technologies. This work suggests that the focus of diet formulation strategies should be on reducing the total nitrogen content of the

Table 6. Sensitivity of the Lin-pH and Exp-pH Models to the input variables.

			Lin-pH model sensitivity		Exp-pH Model sensitivity	
Variable (Mean)	Value	Value relative to mean (%)	ES (g h^{-1})	% change	ES (g h^{-1})	% change
Average		100	0.158		0.115	
Tfilm	293	80	0.121	−24	0.065	−44
(298 K)	296	90	0.138	31	0.086	−25
	301	110	0.181	14	0.152	32
	303	120	0.207	31	0.200	74
v	0.020	80	0.141	−11	0.096	−16
(0.025 m s–1)	0.023	90	0.150	−5	0.105	−8
	0.028	110	0.166	5	0.124	8
	0.030	120	0.173	10	0.133	16
TAN	0.40	80	0.134	−15	0.092	−20
(0.5 mol L–1)	0.45	90	0.155	−2	0.115	1
	0.55	110	0.188	19	0.158	38
	0.60	120	0.209	32	0.192	68
PH	7.0	80	0.117	−26	0.002	−98
(8.8)	7.9	90	0.137	−13	0.016	−86
	9.7	110	0.179	13	0.602	426
	10.6	120	0.199	26	1.372	1098

resulting urine and feces, and perhaps less on reducing the manure pH properties.

SUMMARY

A model was developed to simulate the NH_3 emission from pig slurry of varying composition. The new model was built from preexisting E_s models, and then calibrated and validated with manure collected from grower-finisher pigs fed various diets that resulted in slurry samples with a range of TAN concentrations (0.3 to 1.1 mol L^{-1}) and pH (8.3 to 9.1) measurements. The bias in E_s simulations compared with measured results was -3% using the new model, compared with -39% using a preexisting model format, and this improvement is attributed to the improvement in estimating the amount of NH_3 relative to TAN in the slurry.

During model calibration, the amount of NH_3 relative to TAN was between 3 and 9%. A linear regression equation was developed to relate the fraction (f) of NH_3 relative to the TAN of the slurry to the slurry TAN concentration and mixed slurry pH, a change from exponential relationships between f and pH in existing models. It is suggested that the NH_3 may have become a buffer for the solution between pH 8.5 and 10.5, thus reducing the amount of NH_3 relative to TAN available for emission, and that predicted by the K_a-based exponential f model. The average emission box NH_3 concentration simulated with the model was less than 25% different from the average measured box NH_3 concentration, a significant improvement over simulations using previous model equations where the average simulated and measured concentration values differed between 17 and 137%. There was increased lack of fit between measured and simulated concentration levels when the slurry exhibited TAN or pH values that were at or near the range of values used in the model development. More measurements with diluted slurry will help uncover the minimum amount of NH_3 in a slurry sample that is in volatile form.

ACKNOWLEDGEMENTS

The assistance provided by Ms. Laura Smith, Ms. Karen Stewart and Mr. Rob Fengler during data collection is appreciated. The authors acknowledge the financial support provided by NSERC. Also, SaskPork, Alberta Pork, Manitoba Pork and Saskatchewan Agriculture and Food Development Fund provided strategic funding for the Prairie Swine Centre Inc.

REFERENCES

Aarnink, A.J.A. and A. Elzing. 1998. Dynamic model for ammonia volatilization in housing with partially slatted floors, for fattening pigs. *Livestock Production Science* 53: 153–169.

Anderson, G.A., R.J. Smith, D.S. Bundy and E.G. Hammond. 1987. Model to predict gaseous contaminants in swine confinement buildings. *Journal of Agricultural Engineering Research* 37: 235–253.

Arogo, J., P.W. Westerman and Z.S. Liang. 2003. Comparing ammonium ion dissociation constants in swine anaerobic lagoon liquid and deionized water. *Transactions of the ASAE* 46(5): 1415–1419.

ASTM. 2003. ASTM Standard D 5157 – 97 (Reapproved 2003). Standard guide for statistical evaluation of indoor air quality models. In Annual Book of ASTM Standards. West Conshohocken, PA: American Society of Testing and Materials.

Canh, T.T., A.J.A. Aarnink, J.B. Schutte, A. Sutton, D.J. Langhout and M.W.A. Verstegen. 1998a. Dietary protein affects nitrogen excretion and ammonia emission from slurry of growing-finishing pigs. *Livestock Production Science* 56: 181–191.

Canh, T.T., A.J.A. Aarnink, M.W.A. Verstegen and J.W. Schrama. 1998b. Influence of dietary factors on the pH and ammonia emission of slurry from growing-finishing pigs. *Journal of Animal Science* 76: 1123–1130.

Harper, L.A., R.R. Sharpe and T.B. Parkin. 2000. Gaseous nitrogen emissions from anaerobic swine lagoons: Ammonia, nitrous oxide, and dinitrogen gas. *Journal of Environmental Quality* 29(4): 1356–1365.

Haslam, R.T., R.L. Hershey and R.H. Keen. 1924. Effect of gas velocity and temperature on rate of absorption. *Industrial and Engineering Chemistry* 16(2): 1224–1230.

Incropera, F.P. and D.P. DeWitt. 1996. *Fundamentals of Heat and Mass Transfer*, 4th edition. New York, NY: John Wiley & Sons.

Jayaweera, G.R. and D.S. Mikkelsen. 1990. Ammonia volatilization from flooded soil systems: A computer model. I. Theoretical aspects. *Soil Science Society of America Journal* 54: 1447–1455.

Lewis, W.K. and W.G. Whitman. 1924. Principles of gas absorption. *Industrial and Engineering Chemistry* 16(12): 1215–20.

Liang, Z.S., P.W. Westerman and J. Arogo. 2002. Modeling ammonia emission from anaerobic swine manure. *Transactions of the ASAE* 45: 787–798.

Liss, P.S. and P.G. Slater. 1974. Flux of gases across the air-sea interface. *Nature* 247(5464): 181–184.

Ni, J.Q. 1999. Mechanistic models of ammonia release from liquid manure: A review. *Journal of Agricultural Engineering Research* 72: 1–17.

Ni, J.Q., J. Hendricks, C. Vinckier and J. Coenegrachts. 2000. Development and validation of a dynamic model of ammonia release in pig house. *Environment International* 26: 105–115.

Paul, J.W. and E.G. Beauchamp. 1989. Relationship between volatile fatty acids, total ammonia and pH in manure slurries. *Biological Wastes* 29: 313–318.

Sawyer, C.N. and P.L. McCarty. 1978. *Chemistry for Environmental Engineering*, 3rd edition. Toronto, ON: McGraw-Hill Book Company.

Smith, L.F., S.P. Lemay, J.F. Patience and R.T. Zijlstra. 2004. Effects of dietary crude protein level and sugarbeet pulp inclusion on nitrogen excretion patterns in grower and finisher pigs. *Canadian Journal of Animal Science* 84(4): 717–720.

Sommer, S.G. and S. Husted. 1995. A simple model of pH in slurry. *Journal of Agricultural Science* 124: 447–453.

Treybal, R.E. 1980. *Mass Transfer Operation*, 3rd edition. Toronto, ON: McGraw-Hill Book Company.

Welty, J.R., C.E. Wicks and R.E. Wilson. 1984. *Fundamentals of Momentum, Heat and Mass Transfer*, 3rd edition. Toronto, ON: John Wiley & Sons.

Zhang, R.H., D.L. Day, L.L. Christianson and W.P. Jepson. 1994. A computer model for predicting ammonia release rates from swine manure pits. *Journal of Agricultural Engineering Research* 58: 223–229.

LIST of SYMBOLS

φ	ion activity coefficient
υ	kinematic viscosity ($m^2\ s^{-1}$)
A	surface area (m^2)
A	line of regression intercept
B	line of regression slope
C_B	ammonia concentration of the emission box headspace (mol L^{-1})
C_G	ammonia concentration of the gas film at the liquid surface (mol L^{-1})
C_H	ammonia concentration of the slurry pit headspace (mol L^{-1})
C_L	ammonia concentration of the liquid (mol L^{-1})
C_R	ammonia concentration of the room (mol L^{-1})
$D_{A,B}$	diffusivity of substance A in substance B ($m^2\ s^{-1}$)
E_S	NH_3 emission rate from slurry (mol s^{-1})
EC	electrical conductivity (mS cm^{-1})
$F_{A,B}$	statistical influence of an effect with A degrees of freedom compared to the mean square error with B degrees of freedom
f	fraction of TAN in the form of ammonia
FB	fractional bias
FS	bias based on the variance
H	Henry's Law constant [$(\text{mol } L^{-1})_{Liquid}/(\text{mol } L^{-1})_{Gas}$]
H'	Henry's Law constant [atm/(mg L^{-1})]
H''	Henry's Law constant [$(\text{mol } L^{-1})_{Gas}/(\text{mol } L^{-1})_{Liquid}$]
H^+	hydrogen ion concentration (mol L^{-1})
HPC	high protein diet
HPSBP	high protein diet with sugarbeet pulp
K_a	dissociation constant
k	convective mass transfer coefficient ($m\ s^{-1}$)
k_G	gas film mass transfer coefficient ($m\ s^{-1}$)
k_L	liquid film mass transfer coefficient ($m\ s^{-1}$)
LPC	low protein diet
LPSBP	low protein diet with sugarbeet pulp
N	number
NH_3	Ammonia
NH_4^+	ammonium
NMSE	normalized mean square error
P_G	equilibrium partial pressure of ammonia in air (atm)
P_{CO}	proportionality coefficient
pH	negative log of the hydrogen ion concentration
Q_B	emission box air exchange rate ($L\ s^{-1}$)
Q_H	slurry pit air exchange rate ($L\ s^{-1}$)
q	pH change coefficient
R	correlation coefficient
Re	Reynolds Number
Sc	Schmidt Number
T	slurry temperature (K)
T_c	slurry temperature (°C)
T_{film}	film temperature (K)

TAN	mass of nitrogen contained within ammonia and ammonium molecules in solution (mol L^{-1})
V_B	emission box headspace volume (L)
V_H	slurry pit headspace volume (L)
V	air velocity (m s^{-1})